Trans. JWRI, Vol. 22 (1993), No. 2

Weld HAZ Toughness and Its Improvement of Low Alloy Steel SQV-2A for Pressure Vessels (Report 1)†

– Effect of cooling time on microstructure and Charpy impact value in single thermal cycle –

Fukuhisa MATSUDA*, Kenji IKEUCHI and Jinsun LIAO*****

Abstract

The microstructures and Charpy impact properties of weld HAZ of low alloy steel SQV-2A were investigated with particular reference to the effects of the formation of M-A constituent and its morphology. The weld HAZ thermal cycles having different cooling times $\Delta t_{8/5}$ were simulated with the Gleeble 1500 thermal/mechanical simulator. The formation of M-A constituent and its morphology were examinated by TEM technique and two stage electrolytic etching method. For this steel, M-A constituent began to form at 20 s of cooling time $\Delta t_{8/5}$, and it coexisted with upper bainite and even lower bainite over a wide range of cooling time $\Delta t_{8/5}$. With increasing in cooling time, the M-A constituent formed not only near the grain boundary but also in bulk region, and changed from elongated shape to massive shape. Both enlongated M-A constituent and massive M-A constituent seem to impair the HAZ toughness of SQV-2A steel. The M-A constituent acts as the initiation site of microcracking to induce the loss of absorbed energy of Charpy impact test, but the absorbed energy of Charpy impact test may be affected by not only the M-A constituent but also the matrix, because the matrix itself became brittle with increasing in cooling time.

KEY WORDS: (Weld HAZ) (Cooling Time $\Delta t_{8/5}$) (Impact Property) (M-A Constituent) (Carbon Diffusion)

1. Introduction

Embrittlement of the weld HAZ (Heat Affected Zone) of low alloy steels has absorbed much attention for decades, because it induces unexpected failure of joints and occasionally leads to the destruction of the whole welded constructions such as pressure vessels, ships and bridges. Therefore, a great deal of studies have been carried out on the toughness of weld HAZ until now. It has been reported that the toughness of weld HAZ is affected by many factors such as prior austenite grain size, microstructures, non-metallic inclusion, martensite-austenite (M-A) constituent and dislocation density.[1-3] Recently, large attention has been paid to the M-A constituent which was observed in the high heat-input weld HAZ. According to these investigations, the M-A constituent is very hard, and probably acts as the initiation site of crack.[4-7] Besides, the formation condition, element distribution and the internal structure of M-A constituent have also been studied.[8-13] However the steels used in these studies have very low carbon content (lower than 0.15 mass%).

Low alloy steel SQV-2A has been widly employed to build pressure vessels because of its superior low-temperature toughness and weldability, but like other low alloy steels, its weld HAZ may lose toughness, especially when high heat-input welding process is adopted. The carbon content of this steel is about 0.19 mass%, higher than those of the low alloy steels studied before.[8-13] Therefore, we think that the formation and decomposition of the M-A constituent in this steel and its effect on toughness will be appreciably diferent from those in the steels studied in previous investigations, since the formation of M-A constituent is suggested to be influenced by the carbon content.[8] Therefore, we carried out the study about the behaviour of M-A constituent in SQV-2A steel and its influence on toughness.

† Received on December 20, 1993
* Professor
** Associate Professor
*** Graduate Student

Transactions of JWRI is published by Welding Research Institute, Osaka University, Ibaraki, Osaka 567, Japan

In this paper, Gleeble 1500 was used to simulate the thermal cycles of weld HAZ with different heat-inputs. Then factors controlling the toughness of the simulated weld HAZ were systematically investigated with particular reference to the M-A constituent. The effects of other factors such as prior austenite grain size and facet size were also discussed. Toughness was evaluated by absorbed energy of V-notch Charpy impact test at the temperature of 293K.

2. Experimental details

2.1 Experimental material

The chemical composition of the steel SQV-2A used is shown in **Table 1**. The as-received steel was a quenched and tempered plate. The plate thickness is about 200 mm.

Table 1 Chemical composition of experimental steel used

Material	Chemical composition (mass%)						
	C	Si	Mn	P	S	Ni	Mo
SQV-2A	0.19	0.24	1.48	<0.01	<0.01	0.62	0.56

2.2 HAZ simulation and Charpy test

As shown in **Fig. 1**, samples (10x10x55 mm) for thermal cycle simulation were cut with the longest side parallel to the rolling direction at positions of 1/4t or 3/4t. The Gleeble 1500 thermal/mechanical simulator was used to simulate the weld thermal cycles of the coarse grained HAZ (CGHAZ). The simulated thermal cycles are schemetically shown in **Fig. 2**. A peak temperature of 1623 K was chosen, and the holding time

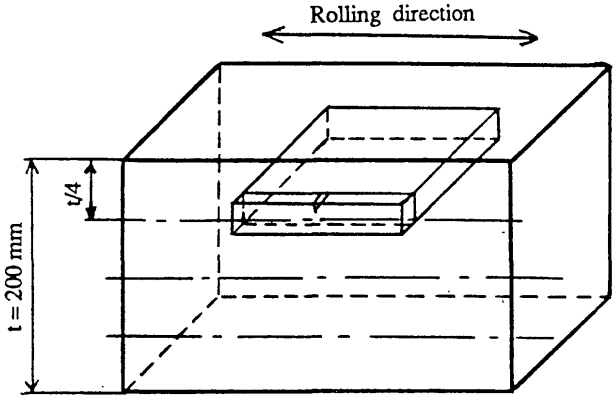

Fig. 1 Schematic diagram of samples

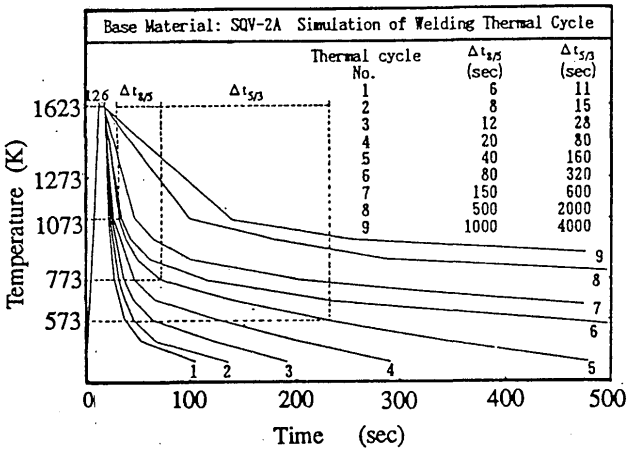

Fig. 2 Thermal cycle used

at the peak temperature was 6 s. In order to simulate the weld HAZ with different heat-input, cooling time from 1073 to 773K ($\Delta t_{8/5}$) was varied from 6 to 1000s, because the microstructure of the CGHAZ has been said to be controlled by the cooling time from 1073 to 773K. After the weld HAZ thermal cycle was applied, a V notch 2 mm in depth was machined, and the notched specimen was subjected to the Charpy impact test to evaluate the toughness of simulated HAZ. For convenience, absorbed energy at 293K was employed as a measure of HAZ toughness.

2.3 Metallography and hardness measurement

For optical microscopy, polished specimens were etched in 2% Nital. The replica technique and thin foil technique were also used to investigate the formation of upper bainite and M-A constituent by TEM observation. In order to observe the type, size, formation and decomposition of M-A constituent with SEM, two stage electrolytic etching method was used, by which ferrite and carbide will be etched preferentially in the 1st and 2nd stages respectively.[9] The fraction of M-A constituent was calculated from the area of M-A constituent. Fracture surfaces were also examinated by SEM. Hardness was measured with Vickers hardness tester (9.8 N load).

3. Results and discussion

3.1 Relations of toughness and hardness of weld HAZ with cooling time $\Delta t_{8/5}$

The relations of absorbed energy and hardness of weld HAZ with cooling time $\Delta t_{8/5}$ are shown in **Fig. 3**. With increasing cooling time $\Delta t_{8/5}$, the absorbed energy was generally decreased, although it was slightly

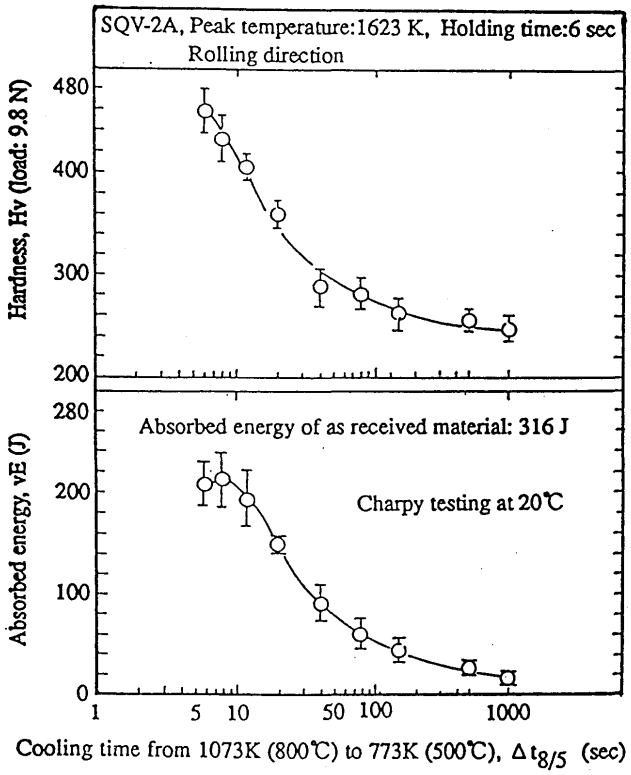

Fig. 3 Relations of absorbed energy and hardness with cooling time $\Delta t_{8/5}$

increased with increasing $\Delta t_{8/5}$ from 6 to 8 s. When $\Delta t_{8/5}$ is larger than 150 s, the reduction of the absorbed energy tends to be saturated. Hardness was decreased monotonously with increasing cooling time $\Delta t_{8/5}$ from 6 to 1000s. Thus, low heat-input welding is preferred in order to obtain better toughness, but even in the case of 8 s of $\Delta t_{8/5}$, the absorbed energy is still lower than the absorbed energy of the base metal. Moreover, when cooling time is short, the hardness is much higher than that of the base metal (about 205Hv), suggesting that the susceptibility to cold cracking may be very high. Therefore, the heat treatment such as PWHT (Post Weld Heat Treatment) or temper bead is necessary to improve the toughness and to eliminate the danger of cold cracking.

3.2 Relation between microstructure and cooling time $\Delta t_{8/5}$

Typical microstructures at different cooling times are shown in **Fig. 4**. In this paper, bainite is classfied as lower bainite and upper bainite according to the classical classification by morphology of carbide, i.e. lower bainite and upper bainite are lath ferrite with intra-lath and inter-lath carbide precipitation respectively. For the cooling times $\Delta t_{8/5}$ in the range of 6 to

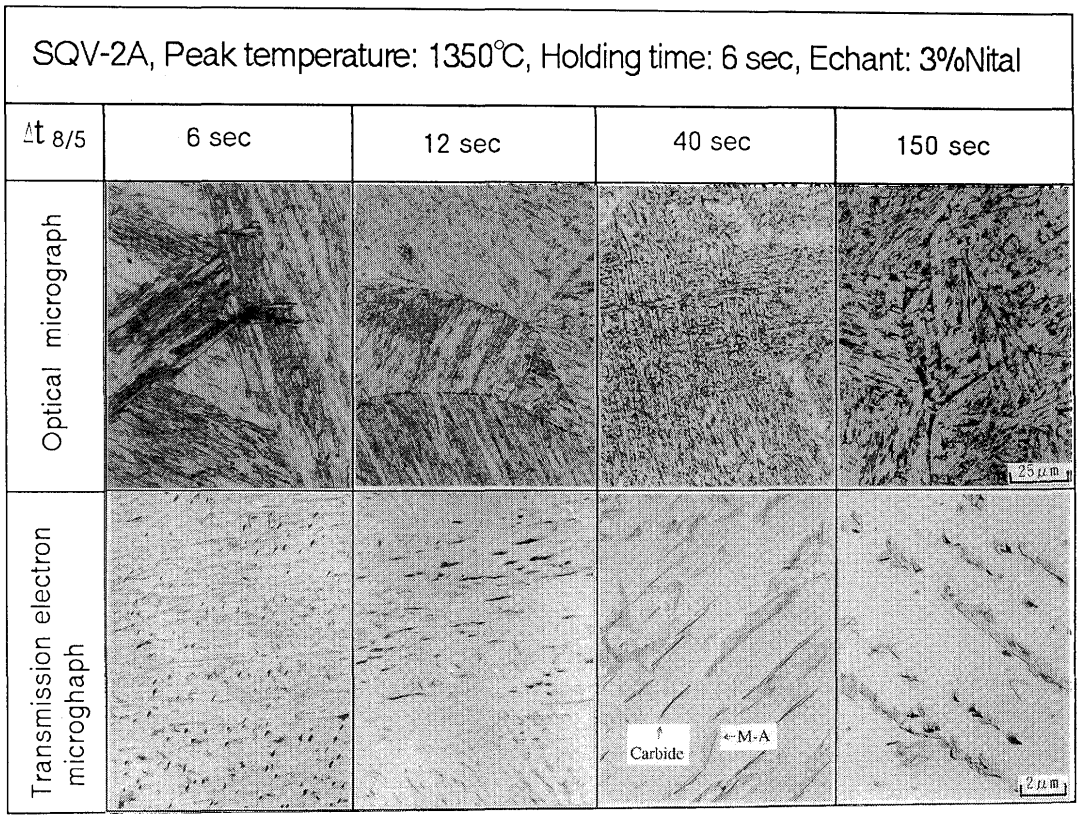

Fig. 4 Typical microstructures at different cooling time $\Delta t_{8/5}$

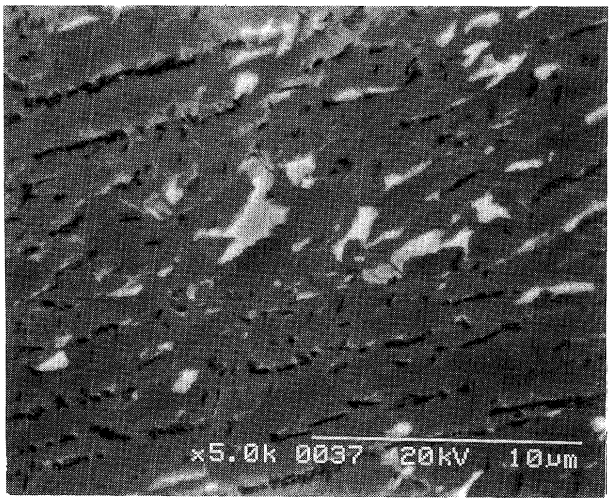

Fig. 5 Microstructures at the cooling time $\Delta t_{8/5}$ of 40 s (Etched with two stage electrolytic etching method)

8 s, the microstructure consists mainly of martensite and lower bainite. Upper bainite was observed from 12 s of $\Delta t_{8/5}$, and the M-A constituent was observed from 20 s of $\Delta t_{8/5}$. When cooling time $\Delta t_{8/5}$ is 40 s, microstructures consist of lower bainite, upper bainite, M-A constituent and bainitic ferrite, as shown in **Fig. 5**. With increasing cooling time, the amounts of lower bainite and upper bainite were decreased, and M-A constituent and bainitic ferrite were increased. When $\Delta t_{8/5}$ is over 150 s, microstructures are almost M-A constituent and bainitic ferrite, and the ferrite-carbide structure decomposed from carbon-enriched austenite can also be observed. Proeutectoid ferrite was not observed for $\Delta t_{8/5}$ less than 1000 s. The variance of microstructures can be qualitatively illustrated in **Fig. 6**.

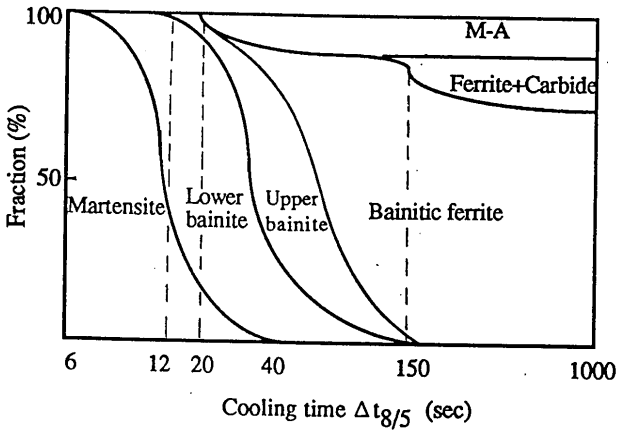

Fig. 6 Variance of microstructures with cooling time $\Delta t_{8/5}$

3.3 Morphology of M-A constituent at different cooling time

From the results of observation by both two stage electrolytic etching method and TEM technique, the M-A constituent is believed to form beginning from 20s

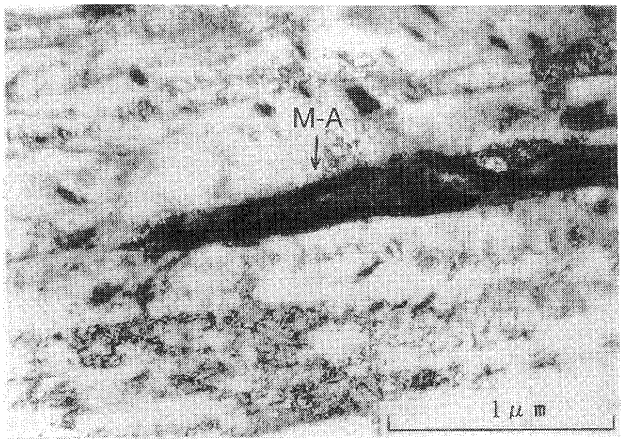

Fig. 7 Image of M-A constituent by TEM observation ($\Delta t_{8/5}$ = 20 s)

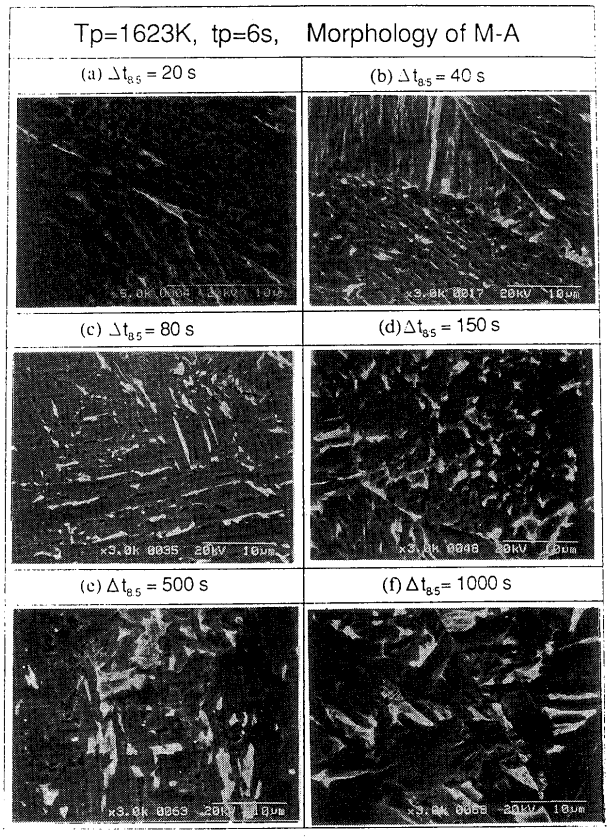

Fig. 8 Variance of the morphology of M-A constituent with cooling time $\Delta t_{8/5}$

of $\Delta t_{8/5}$. **Fig. 7** shows a thin foil image which can be regarded as an example of M-A constituent.

Variance of morphology of M-A with different cooling time $\Delta t_{8/5}$ is shown in **Fig. 8**. As can be seen from Fig. 8, the M-A constituent formed mostly near the prior austenite grain boundary for the cooling times $\Delta t_{8/5}$ in the range of 20 to 40 s, but in the range of 80 to 1000 s, M-A constituent formed in the bulk region.

According to F. Matsuda et al.,[8] M-A constituent can be classified morphologically into enlongated M-A constituent and massive M-A constituent. For this steel, most of M-A constituents belong to enlongated type for $\Delta t_{8/5}$ less than 80 s, but for $\Delta t_{8/5}$ over 80 s most of them belong to massive type. As shown in **Fig. 9**, the enlongated M-A formed between two ferrite laths, and massive M-A formed among three or more ferrite laths.

For cooling times $\Delta t_{8/5}$ in the range from 150 to 1000 s, ferrite-carbide structures were observed, as can be seen from Fig. 8(e). The authors think that they might be formed by the decomposition of carbon enriched austenite islands, which could transform to M-A constituents if the cooling rate was not so slow.

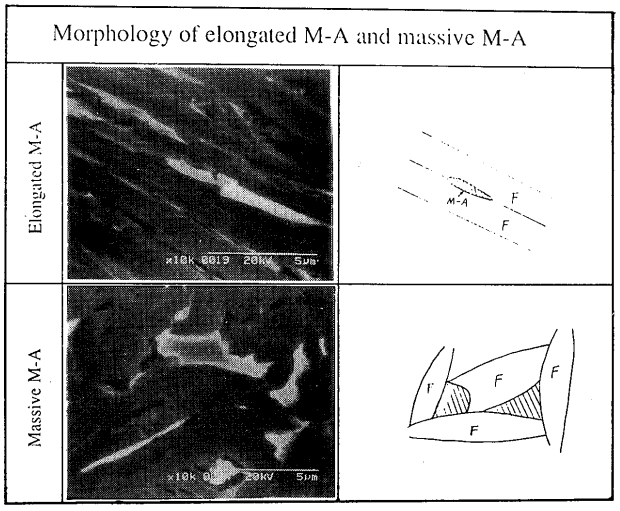

Fig. 9 Morphologies of elongated M-A constituent and massive M-A constituent

3.4 Effect of carbon content on the formation of M-A constituent and microstructure

It can be seen from Figs. 6 and 8 that M-A constituent coexists with upper bainite and lower bainite over a wide range of cooling times $\Delta t_{8/5}$ from 20 to 150 s

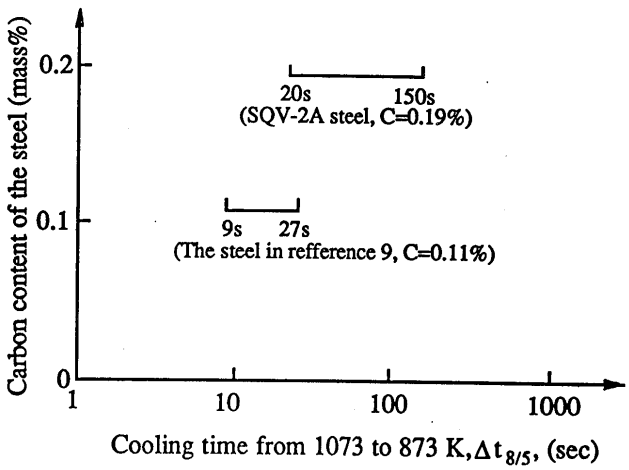

Fig. 10 The range of cooling time $\Delta t_{8/5}$ for the coexistence of M-A constituent with upper bainite and lower bainite

for SQV-2A steel, and the ferrite-carbide structure will be observed when $\Delta t_{8/5}$ is over 150 s. In comparison with this, the coexistence of M-A constituent with lower and upper bainite has been observed in a narrow range of cooling times $\Delta t_{8/5}$ from 9 to 27 s for the steel studied by H. Ikawa etal.,[9] as shown in **Fig.10**. This difference is apparently due to the different chemical compositions especially different carbon contents, which are 0.19 and 0.11 mass% respectively.

In order to explain the coexistence of M-A constituent with upper bainite and lower bainite, we should pay attention to the mechanism of bainite transformation. Three theories have been proposed to interpret the mechanism of bainite transformation:[16]

(i) supersaturated ferrite theory;

(ii) carbon diffusion theory;

(iii) theory of carbide precipitation at the γ/α interface.

For supersaturated ferrite theory, many negative opinions have been suggested,[17] and by this theory the coexistence of M-A constituent with bainite can not be explained, because the prerequisite for the formation of M-A constituent is the carbon concentration.[8]

The carbon diffusion theory assumes that since the solubility of carbon in α phase is much smaller than in γ phase, carbon has to flow out of α phase into γ phase at the γ/α transformation interface. Therefore, carbon concentration will build up in γ phase in front of the advancing γ/α interface.

The theory of carbide precipitation at the γ/α interface assumes that carbides precipitate in the carbon concentrated region and the decrease in the carbon content around the precipitated carbide provides a driving force for transformation from γ to α.

Both the carbon diffusion theory and the theory of carbide precipitation at the γ/α interface have a common idea, i.e. the carbon diffusion at the γ/α interface. According to this idea, the coexistence of M-A constituent with upper bainite and lower bainite can be explained as follows.

The distribution of carbon content at the γ/α interface can be expressed by **Fig.11**. When cooling rate is fast (for $\Delta t_{8/5}$ less than 20 s), the γ/α interface moves rapidly and the transformation temperature is comparatively low, so that the long range diffusion of carbon from the interfacial region into interior of γ phase is difficult. As a result, high carbon content probably build up at the γ/α interface, and the carbide precipitation is promoted. For this reason, lower bainite and upper bainite were observed at short cooling times $\Delta t_{8/5}$. However, with decreasing in cooling rate (or increasing in cooling time $\Delta t_{8/5}$ from 20 to 150 s), the γ/α interface advances slowly and the transformation temperature becomes comparatively high, so that long range diffusion of carbon becomes possible, and more carbon atoms can diffuse into the interior of γ phase from the concentrated region. As a result, the carbon concentration at the γ/α interface will be reduced, and the formation of carbide will become difficult. Thus carbon enriched austenite islands will remain, and these island-lik carbon enriched austenites may be transformed to M-A constituents at lower temperature if the cooling rate is not too slow. From the above discussion, it can be easily understood that in a certain range of cooling rate, the M-A constituent can coexists with bainite. With decreasing the cooling rate, the amount of bainite is decreased and the amount of M-A constituent is increased. (see Fig. 4)

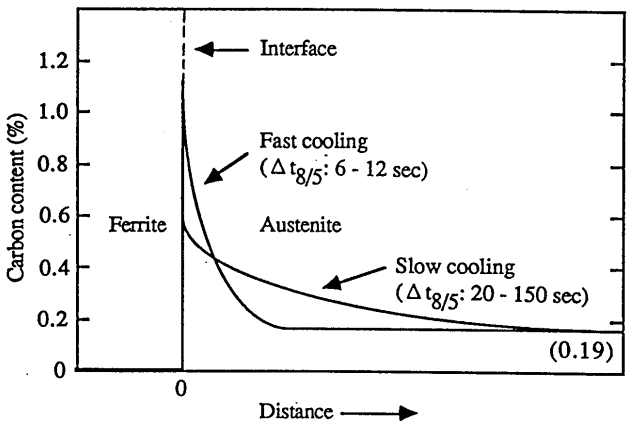

Fig. 11 Carbon distribution at the γ/α interface

For the steel of high carbon content, even at slow cooling rate, the carbon concentration building up at γ/α interfaces is relatively high, so that carbide can form at the interface. However, if the carbon content of the steel is low, the carbon concentration building up at the interface is also low, so the carbide precipitation become different. In order to form the carbide precipitation faster cooling rate is needed, because the carbon concentration at γ/α region will become high at faster cooling rate. This is probably a reason why M-A constituent coexists with upper and lower bainite over a wider range of cooling time $\Delta t_{8/5}$ for SQV-2A steel.

As can be seen from Fig. 8, for cooling time $\Delta t_{8/5}$ from 20 to 40 s, the M-A constituent was formed mainly near the prior austenite grain boundary, and the microstructures in the interior of the grain consist almost of lower bainite and upper bainite. This is because the transformation temperature near the prior austenite grain boundary is somewhat higher than in the interior of the grain. Since the γ/α transformation proceeds at higher temperature near the prior austenite grain boundary, long range diffusion of carbon is possible, thus the M-A constituent can form.

When the cooling rate is further decreased (for $\Delta t_{8/5}$ longer than 150 s), although the carbon content of austenite at the γ/α interface is not very high, the average carbon content in the interior of carbon enriched austenite island will become higher, since more carbon atoms can diffuse into the interior of austenite island from the γ/α interfacial region. In carbon enriched austenite island, the carbide will nucleate and grow, provided that the carbon enriched austenite island is kept at comparatively high temperature for a long time.

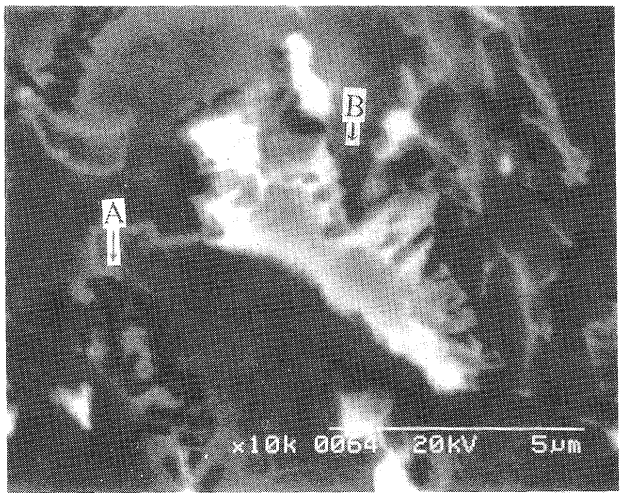

Fig. 12 Ferrite-carbide structures (A) and partially decomposed M-A constituent (B)

Therefore, carbide precipitates in the interior of austenite islands as the cooling rate is further decreased, which leads to the decomposition of carbon-riched austenite islands into ferrite-carbide structures, as shown in **Fig. 12.** It should be noted that in some cases only the edge region of carbon-riched austenite island was decompoed into carbide because of somewhat higher carbon content in edge region, while the centre region of the island was transformed to M-A constituent.

3.5 Effect of microstructures on the HAZ toughness

As shown in Fig. 3, the absorbed energy of the Charpy impact test began to be decreased drastically at the cooling time $\Delta t_{8/5}$ of 20 s, and at this cooling time, the M-A constituent began to form. Therefore, the authors pay attention to the M-A constituent. Just as reported in previous studies,[4-7] the authors have also observed that M-A constituent acts as the initiation site for cracking, as shown in **Fig. 13.** In order to investigate the effect of the amount of the M-A constituent on the toughness, the area fraction of M-A constituent was measured at different cooling times. As shown in **Fig. 14(a),** the area fraction of M-A constituent was increased with increasing in cooling time $\Delta t_{8/5}$. The relationship between area fraction of M-A and absorbed energy is shown in **Fig. 14(b).** With increasing in the area fraction of M-A constituent, absorbed energy was reduced.

Okada et al. have suggested that for HSLA steels of lower carbon content, the elongated M-A constituent has only slight influence on the toughness, while the

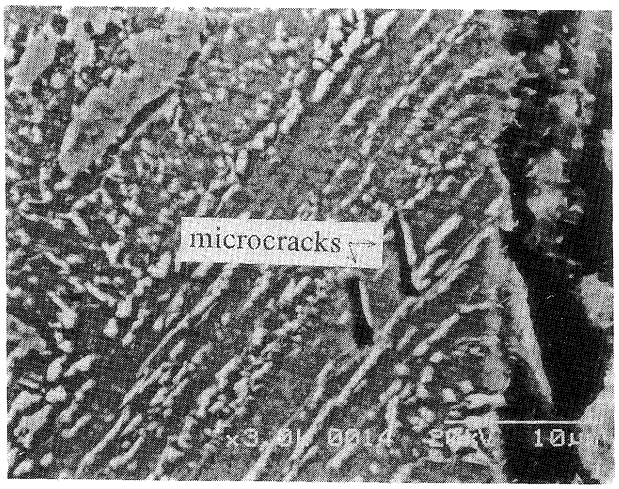

Fig. 13 Microcracks between M-A constituent and matrix

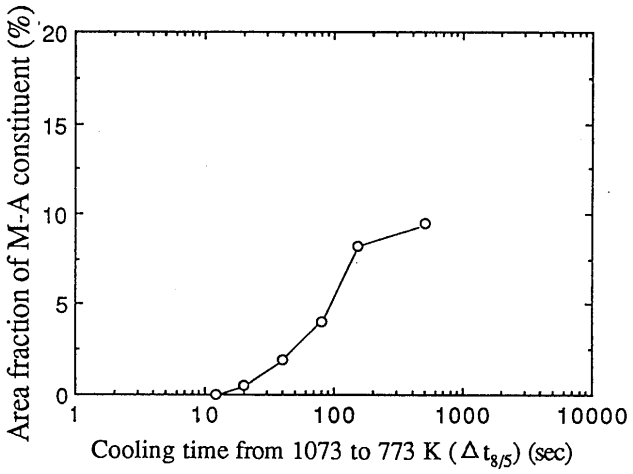

(a)

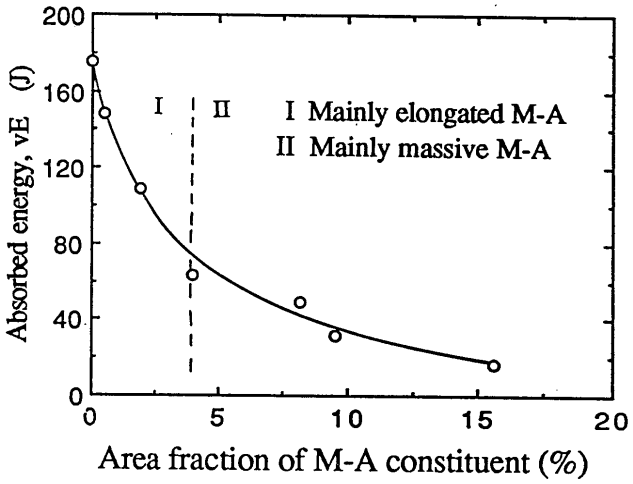

(b)

Fig. 14 (a) Relation of area fraction of M-A constituent with cooling time $\Delta t_{8/5}$
(b) Relation between absorbed energy and area fraction of M-A constituent

massive M-A constituent impairs the toughness seriously. However, it seems that both elongated M-A constituent and massive M-A constituent impair seriously the toughness of SQV-2A steel.

From the finite element analysis of strain field around the M-A constituent under tensile stress, Okada et al. have suggested that

1) a high strain field sets up over wider area around massive M-A constituent than elongated one, and

2) the maximum principal strain around elongated M-A constituent is larger than that around massive one.

From these results, they have concluded that the massive M-A constituent is more detrimental to the toughness of the low carbon HSLA steels than the elongated one probably because the area of strain field

around M-A constituent may be the main factor to affect the initiation of cracking for these low carbon steels.

On the basis of analysis by Okada et al., following two aspects may be the reason why the elongated M-A constituent as well as massive one are detrimental to the toughness of SQV-2A steel.

1) The SQV-2A steel used in present investigation may be regarded as more sensitive to notch, having higher carbon content than the HSLA steels used in Okada's experiments. Therefore, it is conceivable that a smaller crack initiating in the high strain field around the M-A constituent can propagate into the matrix in the SQV-2A steel than the HSLA steels studied by Okada et al..

2) The maximum principal strain around the M-A constituent may also be a controlling facotr for the initiation of cracking.

In fact, both of them probably influence the initiation of cracking for SQV-2A steel.

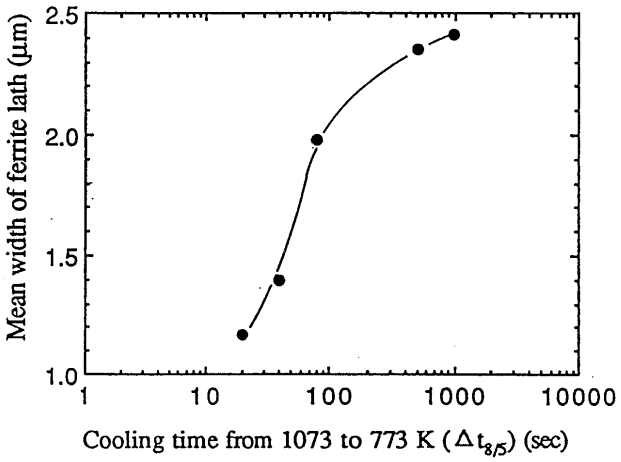

Fig. 15 Relation of mean width of ferrite lath with cooling time $\Delta t_{8/5}$

The absorbed energy of Charpy impact test may be affected not only by the M-A constituent but also by the matrix, because the matrix itself became brittle with increasing in cooling time and might lose the resistance to the propagation of cleavage fracture, behaving as following aspects:

(i) As shown in **Fig. 15**, the width of ferrite lath was increased significantly with increasing in cooling time $\Delta t_{8/5}$ from 20 to 1000 s, implying that the ferrite matrix may become weak. In fact, observation of secondary microcracks shows that microcracks, once initiated, can propagate across the ferrite lath for cooling time $\Delta t_{8/5}$ longer than 80 s, as can be seen in **Fig. 16**.

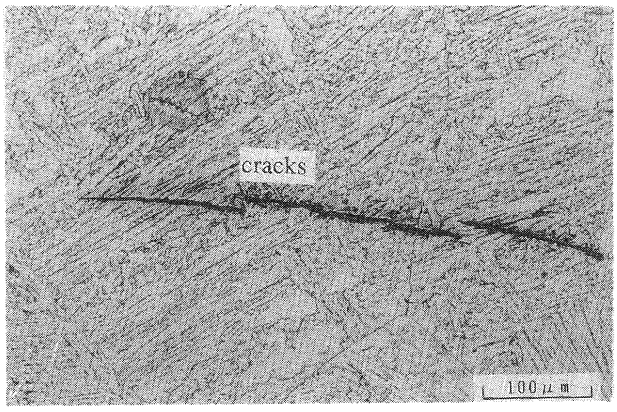

Fig. 16 Microcracks across the ferrite laths

(ii) With increasing in cooling time $\Delta t_{8/5}$, the facet size became larger and larger, and finally closed to the prior austenite grain size, as shown in **Fig. 17**. From the observation of fracture surfaces, it can be seen that the fracture is almost intra-grain cleavage for cooling time $\Delta t_{8/5}$ longer than 40 s. The above facts imply that the interior of the grain have become brittle with increasing in cooling time.

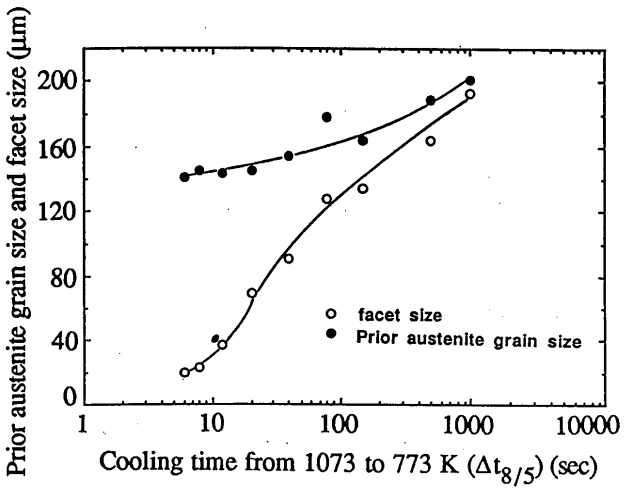

Fig. 17 Relations of prior austenite grain size and facet size with cooling time $\Delta t_{8/5}$

4. Conclusions

In this study, microstructures and Charpy impact properties of simulated weld HAZ of low alloy steel SQV-2A were investigated with particular reference to the effects of the formation and the morphology of M-A constituent. The results can be summarized as follows:

(1) With increasing cooling time $\Delta t_{8/5}$, namely with increasing welding heat-input, the absorbed energy of Charpy impact test of weld HAZ of SQV-2A steel was generally decreased, although it was

slightly increased with increasing cooling time from 6 to 8s. Hardness was monotonously decreased with increasing cooling time from 6 to 1000 s.

(2) With increasing in cooling time $\Delta t_{8/5}$, microstructures changed from martensite and lower bainite to M-A constituent and bainitic ferrite. When $\Delta t_{8/5}$ was longer than 150 s, ferrite-carbide structures were formed from the decomposition of carbon-riched austenite island.

(3) M-A constituent began to form when cooling time $\Delta t_{8/5}$ was 20 s. For the $\Delta t_{8/5}$ in the range of 20 to 40s, M-A formed mainly near the grain boundary; but in the range from 80 to 1000 s, the M-A formed in bulk region. The shape of M-A changed from enlonged shape to massive shape with increasing in cooling time.

(4) Based on the observation of the variance of microstructures with cooling time, the coexistence of M-A constituent with lower bainite and upper bainite can be explained by the use of the proposed mechanisms on bainite transformation.

(5) With increasing in cooling time $\Delta t_{8/5}$, the area fraction of M-A constituent was increased. Absorbed energy of Charpy impact test was decreased with increasing in the area fraction of M-A constituent. The authors think that the absorbed energy of Charpy impact test may be affected not only by M-A constituent but also by matrix, because matrix itself also seems to become brittle with increasing in cooling time.

Acknowledgement

The authors wish to thank Dr. Y. Kikuchi and Dr. T. Kuroda for their useful discussions about the M-A constituent, and also thank Mr. Janak for his cooperation on the TEM observation.

References

1) Makoto SATO and Kazunari YAMATO, "On the Microstructure and Toughness of HAZ in as rolled or Normalized 50 and 60 Kg/mm2 High Strength Steel", Journal of Japanese Welding Society, Vol. 50, No.1 (1981), pp. 11-19 (in Japanese).

2) Junichiro TSUBOI and Yukio HIRAI, "Microstructure and Toughness of Weld Heat Affected Zone in Quenched-Tempered High Strength Steels", Journal of Japanese Welding Society, Vol. 50, No.1 (1981), pp. 28-37 (in Japanese).

3) Yukio HIRAI, "Effect of the Martensite-Austenite Constituent on Toughness of High Strength Steel Weldment", Journal of Japanese Welding Society, Vol. 50, No.1 (1981), pp. 37-46 (in Japanese).

4) C.L. DAVIS and J.E. KING, "Effect of Cooling Time on Intercritically Reheated Microstructure and Toughness in High Strenght Low Alloy Steel", Materials Science and Technology, Vol. 9, Jan. 1993, pp. 8-14.

5) B.C. KIM etal., "Microstructure and Local Brittle Zone Phenomena in High-Strength Low-Alloy Steel Welds", Metallurgy Trans. A, Vol. 22A, Jan. 1991, pp. 139-149.

6) Tetsuya TAGAWA etal., "Influence of Martensitic Islands on Fracture Toughness and Strength of Weld Heat Affected Zone", Iron and Steel, Vol. 79, No. 10 (1993), pp. 48-54 (in Japanese).

7) Tetsuya TAGA WA etal., "Analysis of Embrittlement in Weld Heat Affected Zone due to Formation of Martensitic Islands by Local Criterion Approach", Iron and Steel, Vol. 79, No. 10 1993), pp.55-61 (in Japanese).

8) Fukuhisa MATSUDA etal., "An Investigation on the Behaviour of M-A Constituent in Simulated HAZ of HSLA Steels", IIW Doc. IX-B 1591-90.

9) Hiroshi IKAWA etal., "Effect of Martensite-Austenite Constituent on HAZ Toughness of a High Strength Steel", IIW Doc. IX-1156-80.

10) Ivan HRIVNAK, Fukuhisa MATSUDA and Kenji IKEUCHI, "Investigation of M-A Constituent in High Strength Steel Welds", Trans. of JWRI, Vol. 21, No. 2 (1992), pp. 9-32.

11) Ivan HRIVNAK and Fukuhisa MATSUDA etal., "Investigation of Metallography and Behaviour of M-A Constotuent in Weld HAZ of HSLA Steels", Trans. of JWRI, Vol. 21, No. 2 (1992), pp. 101-110.

12) Hitoshi OKADA, The Thesis for Doctoral Degree of Osaka University, 1993.

13) Yutaka KASAMATSU etal., "Influence of Martensite-Austenite Constituent on Toughenss of Heat Affected Zone of High Strength Weldable Structural Steels", Iron and Steel, Vol. 65, No. 8 (1979), pp. 1222-1231 (in Japanese).

14) F.B. Pickering, Symposium: Transformation and Hardedability in Steels, pp. 109-129, Climax Molybdenum Company of Michigan, AnnArbor, Mich., 1967.

15) V. BISS and R.L. CRYDERMAN, "Matersite and Retained Austenite in Hot-Rolled Low-Carbon Bainitic Steels", Metallurgy Trans., Vol. 2, August 1971, pp. 2267-2276.

16) Y. OHMORI, The Diffusional Transformation of Plain Carbon Steels and the Precipitation of Cementite, Iron and Steel, No. 9 (1971), pp. 124-141 (in Japanese).

17) M. COHEN, Transformation and Hardenability in Steels, Climax Molibdenum Co., (1967), pp.131.